گواهی ارائه مقاله

بدینوسیله گواهی می شود مقاله با عنوان

Simulation of 3-D Cavitation behind a Disk Cavitator using DifferentTurbulence/Mass Transfer Models

باشماره شناسه Aero2014P651T107 توسط جناب آقای محمدرضا پندار

در سیزدهمین کنفرانس انجمن هوافضای ایران (۱۳ الی ۱۵ اسفندماه ۱۳۹۲ - دانشکده علوم و فنون نوین دانشگاه تهران) ارائه شده است.

نویسندگان مقاله: محمدرضا پندار، احسان روحی، امین رحیمی

مهدی فکور

دبیر کنفرانس

Simulation of 3-D Cavitation behind a Disk Cavitator using Different Turbulence/Mass Transfer Models

Amin Rahimi[1], Mohammad Reza Pendar[2], Ehsan Roohi [3]

High Performance Computing, Department of Mechanical Engineering, Ferdowsi University of Mashhad, P.O.Box: 91775-1111, Mashhad, Iran

Abstract

In this paper simulation of cavitating and supercavitating flow behind the three-dimensional disk cavitator is reported. The volume of fluid (VOF) method is applied to track the interface of liquid and vapor phases. Different kinds of turbulence models such as large eddy simulation (LES), $\kappa-\omega$ SST are used. LES turbulence model is the most favored for the cavitation dynamics simulation purposes. Additionally, different types of mass transfer models such as Kunz, Schnerr and Sauer and Zwart were employed. The main innovation in this work is the addition of the Zwart mass transfer model in the OpenFOAM package. Flow at three different cavitation numbers, i.e., σ=0.2, 0.1, and 0.05 is considered. Our numerical results are validated with the experimental data and analytical relations for the cavity length, diameter and drag coefficient and suitable accuracy was observed. it is observed that the most accurate solutions could be obtained if we employ LES turbulence modeling with the Kunz mass transfer model.

Keywords: *Disk cavitator- LES turbulence model- mass transfer model- VOF-Zwart Model*.

Introduction

Cavitation is a multi-phase and complex physical phenomenon which occurs when the local liquid pressure is lower than its saturated vapor pressure [1]. Cavitation usually could appear over marine vehicles such as submarine, torpedoes and marine propeller blades. To increase the performance of the submarines and reduce the viscous drag, some marine vehicles usually needs to be operated in cavitating conditions but one still needs to avoid the negative effects of cavitation such as vibrations, noise and erosion [2].

Cavitation is a 3-dimensional (3-D), unsteady and discontinuous or periodic phenomenon of formation, growth and rapid collapse of bubbles [3]. This process is characterized by a dimensionless number; i.e., $\sigma=(P_\infty-P_v)/0.5\rho U_\infty^2$ called cavitation number [1]. In this equation, P_v is the vapour pressure, ρ is the liquid density, and P_∞, U_∞ are the free stream flow pressure and velocity, respectively. If the velocity of the moving body increases further, the supercavitation will occur which refers to a long cavity that extends more than the body length and closes in the liquid. There is a constant movement of a re-entrant liquid jet in the cavity closure section.

Study of cavitation flow over a three-dimensional geometry disk cavitator has long been of interest to many researchers. Kunz et al. [4] developed a multi-phase computational fluid dynamics technique to model the flow around submerged objects that are exposed to natural cavitation. Their results were presented for the axisymmetric, steady state, transient natural cavitation. Results for the pressure distribute, drag coefficient and cavity shape were compared with the experimental data. Passandideh-Fard and Roohi [5] performed transient 2D/axisymmetric simulations of cavitating flows over disk and cone cavitators. Nouri et al. [6] used a finite volume method to simulate cavitation over a disk, using the Kunz cavitation model and considering LES as the turbulence model. Baradaran-Fard and Nikseresht [7] simulated unsteady 3-D cavitating flows over axisymmetric cavitators. For implementation of the turbulent flow, the shear stress transport, $\kappa-\omega$ SST model was used. Shang et al [8] validated the numerical simulations of cavitating sphere with the experimental data. Roohi et al. [9] used LES turbulence to investigate cavitating flows over hydrofoils using the OpenFOAM package. Morgut et al. [10] compared the Kunz, Zwart and FCM (Full Cavitation Model) mass transfer models using the RANS (Reynolds Averaged Navier Stokes) turbulence equations. The numerical predictions based on the three different tuned mass transfer models are very close to each other and in agreement with the experimental data. Shang [11] simulated cavitation around the cylindrical objects such as submarine within the wide ranges of cavitation numbers from 0.2 to 1.0. $\kappa-\omega$ SST turbulence mode, VOF model and the Sauer mass transfer model was employed to capture the cavitation mechanisms.

In this research, we validated the ability of an open source package, that is, OpenFOAM package to simulate supercavitation flow behind a disk whose experimental, analytical data is available [2]. Volume of fluid (VOF) technique is applied to track the interface of liquid and vapor phases [2]. VOF model used in the OpenFOAM considers the effect of the surface tension force over the free surface. In the current work, we use both of LES and $\kappa-\omega$ SST

1. MSc Graduate
2. MSc Student
3. Assistant Professor, Tel/Fax: 0511-8763304, email: e.roohi@um.ac.ir (corresponding author)

turbulence models to simulate cavitating flows behind a disk. We compared Kunz, Sauer and Zwart mass transfer models. We added the Zwart model to the OpenFOAM package.

Governing Equations

The vapor-liquid flow described by a single-fluid model is treated as a homogeneous bubble-liquid mixture, so only one set of equations is needed to simulate cavitating flows. Thus, starting from the incompressible Navier-Stokes (NS) equations:

$$\partial_t \rho + \nabla.(\rho v) = 0$$
$$\partial_t (\rho v) + \nabla.(\rho v \times v) = -\nabla p + \nabla.s, \quad (1)$$

Eqs. (1) are the governing continuity and momentum equations for a classical RANS and homogeneous mixture multiphase flow. Here, v is the velocity, p is the pressure, $s = 2\mu D$ is the viscous stress tensor, where μ is the viscosity. The rate-of-strain tensor is expressed as

$$D = \frac{1}{2}\left(\nabla v + \nabla v^T\right) \quad (2)$$

Multiphase Flow Modeling

As phase changes from liquid to vapor happens under cavitations, a multiphase flow model has to be employed to describe the flow. Usually, the two-phase mixture governing equation is employed to describe the multiphase flow for cavitation. In this work, we consider a "two-phase mixture" method, which uses a local vapor volume fraction transport equation together with source terms for the mass transfer rate between the two phases due to cavitation.

$$\partial_t \gamma + \nabla.(\gamma \bar{v}) = \dot{m} \quad (3)$$

The mixture density ρ and viscosity μ are defined by:

$$\mu = \gamma\mu_v + (1-\gamma)\mu_l \quad (4)$$
$$\rho = \gamma\rho_v + (1-\gamma)\rho_l \quad (5)$$

where $\dot{m}$ is the mass transfer rate between the phases.

Mass Transfer Modeling

In this work, we employed tree mass transfer models Kunz, Schnerr-Sauer and Zwart. Kunz et al. [12] proposed a semi-analytical cavitation model as follows:

$$\frac{\partial \gamma}{\partial t} + \vec{\nabla}\cdot(\gamma\bar{v}) = \frac{C_{dest}\rho_v Min(P_l - P_v, 0)\gamma}{\rho_l(0.5\rho_l V_\infty^2)t_\infty} + \frac{C_{prod}(1-\gamma)\gamma^2}{\rho_l t_\infty} \quad (6)$$

The first term on the right-hand is steam produced and it Proportional pressure drop from vapor pressure and amount of liquid phase models, while second term is amount of condensation and Proportional to the third power of volume fraction. C_{dest} and C_{prod} are two empirical constants. P_l is liquid filtered pressure and P_v steam pressure. Kunz's model reconstructs the cavity region quite accurately especially in the closure region of the cavity. Therefore we employed Kunz model in the current simulation. Mass transfer model was developed by Schnerr and Sauer [13] as:

$$\dot{m} = -\frac{(1-\gamma)\rho_\vartheta 3\gamma}{R_b} sing(p - p_{sat})\sqrt{\frac{2}{3}(p - p_{sat})/\rho_l} \quad (7)$$

this model is function of bubble numbers per volume unit and bubble diameter calculated. Where R_b is the radius of a bubble, which can be expressed as:

$$R_b = \left(\frac{1}{\frac{4\pi n_0}{3}}\frac{\gamma}{1-\gamma}\right)^{\frac{1}{3}} \quad (8)$$

n_0 is the initial number of bubbles per unit volume.

In Zwart cavitation model et al.[14] Equation (9) is used as a mass transfer equation. Equation divided into two parts, one part for converting liquid phase vapor phase and second part is reversed.

$$\dot{m} = \begin{cases} -Fe\dfrac{3r_{nuc}(1-\alpha)}{R_B}\sqrt{\dfrac{2(P_v - P)}{3\rho_l}} & P < P_v \\ Fc\dfrac{3\alpha\rho_v}{R_B}\sqrt{\dfrac{2(P - P_v)}{3\rho_l}} & P > P_v \end{cases} \quad (9)$$

P_V vapor pressure, r_{nuc} the volume fraction at the core formation, R_B radius of the core formation, F_e,F_c is two empirical coefficients, respectively. Based on reference [10]
$r_{nuc}=5\times10^{-4}$,$R_B=1\times10^{-6}$,$F_{e=}50$,$F_{c=0.01}$

VOF Model

The interface between the liquid and vapor phases is captured by volume of fluid (VOF) method. The VOF equation can be developed from Eq. (3) and described as the following:

$$\frac{\partial \gamma}{\partial t} + \nabla.(\gamma\bar{\upsilon}) + \nabla.[\bar{\upsilon}_c\gamma(1-\gamma)] = 0 \quad (10)$$

The last term on the left-hand side of the above equation is known as the artificial compression term and it is non-zero only at the interface. The compression term stands for the role to shrink the phase-inter phase towards a sharper one. The compression term does not bias the solution in any way and only introduces the flow of γ in the direction normal to the interface. In order to ensure this procedure, Weller suggested the compression velocity to be calculated as:

$$\bar{\upsilon}_c = \min[c_\gamma |\bar{\upsilon}|, \max(|\bar{\upsilon}|)]\frac{\nabla\gamma}{|\nabla\gamma|} \quad (11)$$

In other words, the compression velocity is based on the maximum velocity at the interface. The limitation of v_c is achieved through applying the largest value of the velocity in the domain as the worst possible case. The intensity of the compression is controlled by a constant C_γ, i.e., it yields no compression if it is zero,

a conservative compression for C_γ=1 and high compression for C_γ>1.

Turbulence model

1. LES Model

Large eddy simulation (LES) is based on computing the large, energy-containing structures that are resolved on the computational grid, whereas the smaller, more isotropic, sub-grid structures are modeled. In contrast to RANS approaches, which are based on solving for an ensemble average of the flow properties, LES naturally and consistently allows for medium to small scale, transient flow structures. When simulating unsteady, cavitating flows, it is an important property in order to be able to capture the mechanisms governing the dynamics of the formation and shedding of the cavity [15-16]. The LES equations are theoretically derived, following e.g. Sagaut [17] from Eq. (1). In ordinary LES, all variables, i.e., *f*, are split into grid scale (GS) and sub grid scale (SGS) components, $f = \bar{f} + f'$, where $\bar{f} = G * f$ is the GS component, $G = G(X, \Delta)$ is the filter function, and $\Delta=\Delta(\mathbf{x})$ is the filter width. The LES equations result from convolving the NS with *G*, viz,

$$\begin{aligned} &\partial_t\left(\rho\bar{v}\right)+\nabla.\left(\rho\bar{v}\times\bar{v}\right)=-\nabla\bar{p}+\nabla.\left(\bar{s}-B\right), \\ &\partial_t\rho+\nabla.\left(\rho\bar{v}\right)=0 \end{aligned} \tag{12}$$

Where over-bar denotes filtered quantity. Equation (3) introduces one new term when compared to the unfiltered Eq. (1): the unresolved transport term *B*, which is the sub grid stress tensor. Following Bensow and Fureby [18], *B* can be exactly decomposed as

$$\boldsymbol{B}=\rho.\left(\overline{\bar{v}\times\bar{v}}-\bar{\bar{v}}\times\bar{\bar{v}}+\widetilde{B}\right) \tag{13}$$

, Where now only $\widetilde{B}$ needs to be modeled. The most common subgrid modeling approaches utilizes an eddy or subgrid viscosity, ν_{SGS}, similar to the turbulent viscosity approach in RANS, where ν_{SGS} can be computed in a wide variety of methods. In eddy-viscosity models often,

$$B=\frac{2}{3}\bar{\rho}kI-2\mu k\,\tilde{D}_D \tag{14}$$

Where *k* is the SGS kinetic energy, $\bar{\rho}$ the SGS eddy viscosity, and $\tilde{D}_D$ the SGS eddy diffusivity. In the current study, sub-grid scale terms are modeled using "one equation eddy viscosity" model. In order to obtain *k,* one-equation eddy-viscosity model (OEEVM) uses the following equation:

$$\partial\left(\bar{\rho}k\right)+\nabla.\left(\bar{\rho}k\,\tilde{v}\right)=-B.\tilde{D}+\nabla.(\mu\nabla\mathrm{k})+\bar{\rho}\varepsilon \tag{15}$$

$$\varepsilon=c_\varepsilon k^{3/2}/\Delta \tag{16}$$

$$\mu_\mathrm{k}=c_k\bar{\rho}\Delta\sqrt{k} \tag{17}$$

2. $\kappa-\omega$ **SST model**

In addition to LES, the shear stress Transport (SST) $\kappa-\omega$ model is utilized for turbulence modeling. The $\kappa-\omega$ SST model was developed be Menter to effectively blend the robust and accurate formulation of the $\kappa-\omega$ model in the near-wall region with the free-stream independence of the $\kappa-\varepsilon$ model in the far field. To achieve this, the $\kappa-\varepsilon$ model is converted into a $\kappa-\omega$ formulation. The governing equations are as follow:

Turbulence Kinetic Energy:

$$\begin{aligned} &\frac{\partial}{\partial t}(\rho k)+\frac{\partial}{\partial x_j}(\rho k u_j)=\frac{\partial}{\partial x_j}\left(\left(\mu+\frac{\mu_t}{\sigma_{k3}}\right)\frac{\partial k}{\partial x_j}\right) \\ &+\tau_{ij}\frac{\partial u_i}{\partial x_j}-\beta^*\rho k\omega. \end{aligned} \tag{18}$$

Specific dissipation rate:

$$\begin{aligned} &\rho\frac{\partial\omega}{\partial t}+\rho u_j\frac{\partial\omega}{\partial x_j}=\frac{\partial}{\partial x_j}\left(\left(\mu+\frac{\mu_t}{\sigma_{\omega3}}\right)\frac{\partial\omega}{\partial x_j}\right) \\ &+\frac{\omega}{k}\left(\alpha_3\tau_{ij}\frac{\partial u_i}{\partial x_j}-\beta_3\rho k\omega\right) \\ &+(1-F_1)2\rho\frac{1}{\omega\sigma_{\omega2}}\frac{\partial k}{\partial x_j}\frac{\partial\omega}{\partial x_j}, \end{aligned} \tag{19}$$

Where the coefficients of the model are a linear combination of the corresponding coefficients of the $\kappa-\omega$ and modified $\kappa-\varepsilon$ models as:

$$\begin{aligned} &\left(\psi=F_1\psi_{k\omega}+\left(1-F_1\right)\psi_{k\varepsilon}\right). \\ &k-\omega:\alpha_1=5/9,\beta_1=3/40,\sigma_{k1}=2, \\ &\sigma_{\omega1}=2,\beta^*=9/100, \\ &k-\varepsilon:\alpha_2=0.44,\beta_2=0.0828,\sigma_{k2}=1, \\ &\sigma_{\omega2}=1/0.856,C_\mu=0.09. \end{aligned}$$

The model combines the advantages of the Wilcox $\kappa-\omega$ and the Launder-Spalding $\kappa-\varepsilon$ models, but still fails to properly predict the onset and amount of the flow separation from smooth surfaces, due to the over-prediction of the eddy-viscosity (the transport of the turbulence shear stress is not properly taken into account). The proper transport behavior can be obtained by a limiter added to the formulation of the eddy-viscosity:

$$\mu_t=\rho\frac{k}{\max\left(\omega,SF_2\right)}, \tag{20}$$

Where F_2 is blending function, which restricts the limiter to the wall boundary layer, as the underlying assumptions are not correct for free shear flow. S is an invariant measure of the strain rate. The blending functions F_1 and F_2 are critical to the success of the method.

Simulation Set-up

The total 3D computational domain and boundary conditions are shown in Fig 1. The disk is placed at the center of water tunnel. The two important non-dimensional numbers used are the Reynolds number (Re) and cavitation number σ. U_∞ is the free stream velocity which is imposed 20 m/s. we have

considered different data such as σ=0.2 and Re=5×10^5.

Computational Configuration

The simulation is performed in three dimensions to get a cavitation shape like the experimental data. As the disk is not geometrically complex, we used structured quadrilateral meshes and To save the computational cost , one quarter of the Geometry was considered. Mesh size near the disk is more concentrated. The dimensions of the computational domain are considered according to the experimental data. Tree kinds of grid compared with total 400,000, 900,000, 1,500,000 cells in the domain. Fig. 2 illustrates the mesh which is produced around the disk. The distance between disk and outlet is set as 12D in order to prepare a suitable distance between the outlet and cavity region.

Results and Discussions

Figures 3-5 illustrate a 3D view of the cavitating flow over the disk in $\sigma = 0.2$, 0.1, and 0.05 with LES turbulence model using Kunz and Zwart mass transfer models. Decreasing the cavitation number causes cavity shape shows steady behavior. Length and diameter of cavity increases as cavitation number increases. Kunz model predicts unsteady behavior of cavitation while the Zwart model predicts smooth and regular shape for the cavity.

The contour of volume fraction is illustrated in Figs. 6-8 as a 2D section in the z-plane at $\sigma = 0.2$, 0.1, and 0.05 respectively. Kunz, Sauer and Zwart mass transfer models are compared. The main difference between the models is their re-entrant jets. Length of the re-entrant jet in the Kunz model is shorter than the length in Sauer and Zwart models. Reducing the cavitation number decreases the effect of reentrant jet.

Figure 9 illustrate the contour of pressure, pressure increases at the front of disk due to flow stagnation on the disk, but behind the disk, the flow separates at the sharp edge and the resultant drop in pressure creates a vaporous cavity region. A pressure gradient appears at the interface of vapor phase and liquid phase. This is created due to pressure difference between two phases and is normal to the interface. On the other hand, cavity shedding and condensation of cavity bubbles cause a high pressure variation at the end of cavity region. A sharp interface is visible around the cavity domain which is the result of using VOF model. Pressure levels in Sauer and Zwart models are similar.

Three dimensionless parameters are compared from our simulation with those of experiments and analytical relations, see Tables 1-2 and Figs. 10-12. For validating the present results, the Richardt's semi-empirical relations are selected as the non-dimensional characteristics of the cavity. The relevant formulas for these characteristics are presented by Eqs. (21)-(23). The cavitation number is the main factor in the following formulas [19]

$$\frac{L}{d} = \frac{\sigma + 0.008}{\sigma\left(1.7\sigma + 0.066\right)}\left(\frac{d}{D}\right) \tag{21}$$

$$\frac{d}{D} = \left[\frac{C_D}{\sigma\left(1 - 0.132\sigma^{0.5}\right)}\right]^{0.5} \tag{22}$$

$$C_D = C_{D_0}\left(1 + \sigma\right) \tag{23}$$

L/d and D/d are the ratio of cavity length and cavity diameter to the cavitator diameter, respectively. There are good agreement between the numerical and experimental results in three simulated cavitation numbers. The numerical results have a better agreement with the experimental data comparing with the theoretical predictions. Additionally, drag coefficient (C_D) obtained from the pressure distribution over the disk surface has a good accuracy comparing with the theoretical and experimental results.

The results shows LES turbulence model with the Kunz mass transfer model performs more accurately than $\kappa - \omega$ SST with Sauer, LES with Sauer and finally LES with Zwart. Considering the drag coefficient calculated for the four models, the minimum error is for the LES and Kunz model. Steady supercavity occurs at time of t=40, 60,120 (ms) for cavitation number of σ=0.2, 0.1 respectively. But it occurs few second earlier in Zwart model. At the end of steady supercavity, two behavior are observed :(a) development of reverse liquid flow, (b) separation of very small vapor bubbles into the main stream because of the exit reverse flow into cavity cloud.

Conclusion

In the present study, a finite volume solver benefiting from the VOF interface capturing method , LES or k-ω SST turbulence model and Kunz, Sauer and Zwart mass transfer model has been employed to capture unsteady cavitation and supercavitation flow behind a 3-D disk cavitator in different cavitation numbers, i.e., σ=0.2, 0.1, and 0.05. The simulation is performed under the framework of OpenFOAM. The main innovation in this work is the addition of the Zwart mass transfer model in the OpenFOAM package. Our numerical results are validated with the experimental data and analytical relations for the cavity length, diameter and drag coefficient and suitable accuracy was observed. It is observed that the most accurate solutions will be obtained if we employ LES turbulence modeling with the Kunz mass transfer model.

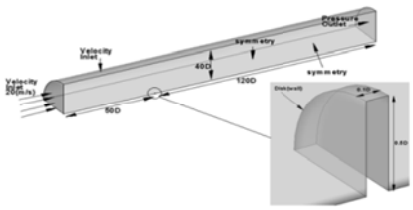

Fig. 1: Computational domain and boundary conditions

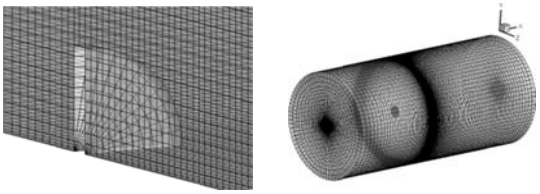

Fig. 2: Mesh generation.

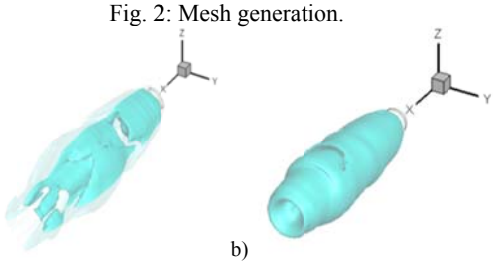

a) b)

Fig. 3: 3D cavitation behind a disk with LES, (a)Kunz(b)Zwart model, $\sigma = 0.2$, t=72(ms).a)

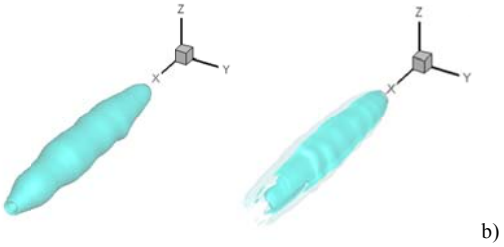

b)

Fig. 4: 3D cavitation behind a disk with LES , (a)Kunz(b) Zwart model, $\sigma = 0.1$,t=80(ms).

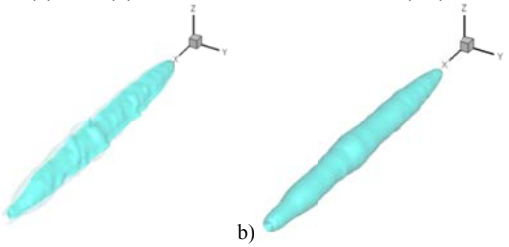

a) b)

Fig. 5: 3D cavitation behind a disk with LES , (b) Kunz(b)Zwart model, σ=0.05, t=187(ms)

(a) Sauer mass transfer model, t=83(ms) (b) Kunz mass transfer model, t=83(ms)

Fig. 6: Contour of vapor phase (cavity region) for σ=0.2

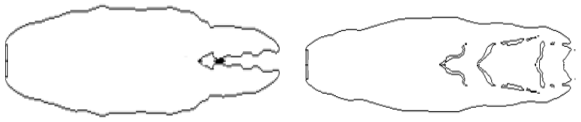

(a) Sauer mass transfer model, t=87(ms) (b) Kunz mass transfer model, t=87(ms)

Fig. 7: Contour of vapor phase (cavity region) for $\sigma = 0.1$

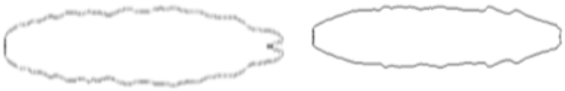

(a) Sauer mass transfer model, t=196(ms) (b) Kunz mass transfer model, t=196(ms)

Fig. 8: Contour of vapor phase (cavity region) for σ=0.05

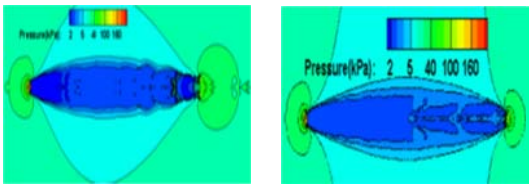

(a)LES, Sauer mass transfer model, t=139(ms) (b) LES, Kunz mass transfer model, t=139(ms)

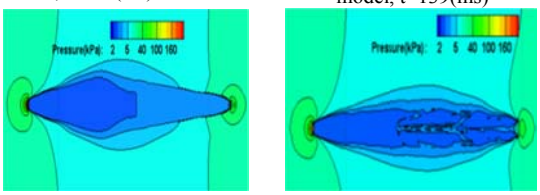

(a)LES, Sauer mass transfer model, t=139(ms) (b) $\kappa-\omega$ SS, Zwart mass transfer model, t=139(ms)

Fig. 9: Contour of pressure for σ=0.05

Table 1: Computed parameters at $\sigma = 0.1$

Method		LES Kunz	LES Sauer	$\kappa-\omega$ SST Sauer	LES Zwart
L/d	Simulation	13.9	17.67	1809	19.64
	Richardt's Theory	14.19	14.19	14.19	14019
	Error	2.04	24.52	33.19	38.40
D/d	Simulation	3.22	2.99	3.59	3.58
	Richardt's Theory	3.1	3.1	3.1	3.1
	Error	3.87	3.55	15.81	15.48
C_D	Simulation	0.85	0.8	0.784	0.749
	Richardt's Theory	0.924	0.924	0.924	18.94
	Error%	8	13.42	15.15	38.7

Table 2: Computed parameters at σ=0.05

Method		LES Kunz	LES Sauer	$\kappa-\omega$ SST Sauer	LES Zwart
L/d	Simulation	32.66	37.74	47.24	46.85
	Richardt's Theory	32.73	32.73	32.73	32.73
	Error	0.21	15.3	44.33	43.14
D/d	Simulation	4.59	4.33	4.72	4.88

	Richardt's Theory	4.26	4.26	426	4.26
	Error	7.75	1.64	10.8	14.55
C_D	Simulation	0.8	0.79	0.791	0.777
	Richardt's Theory	0.882	0.88	0.882	0.882
	Error%	9.3	10.43	10.32	11.9

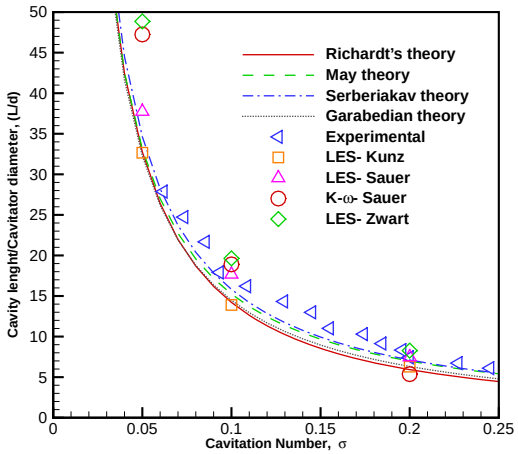

Fig. 10: Comparison of the cavity length/cavitator diameter for different cavitation numbers.

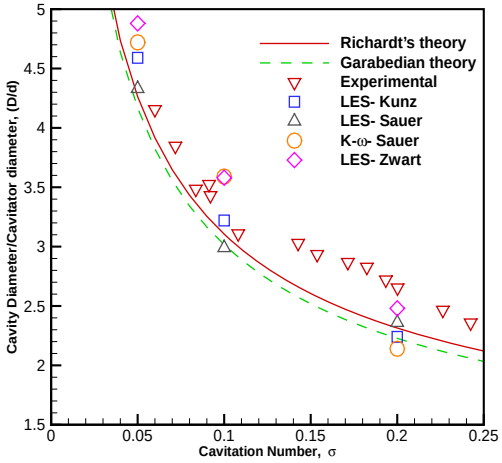

Fig. 11: Comparison of the cavity diameter/cavitator diameter for different cavitation numbers.

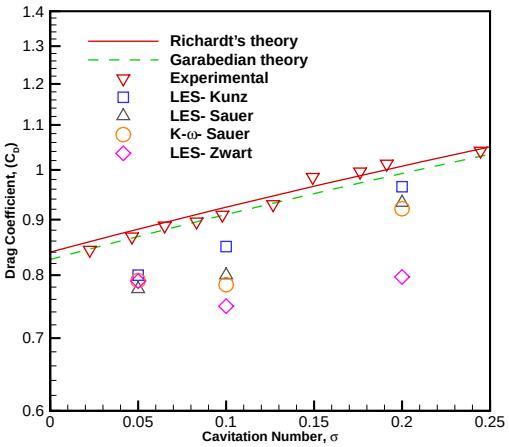

Fig. 12: Comparison of the drag coefficient for different cavitation number.

References

1- Brennen, C.E., Cavitation and Bubble Dynamics, Oxford University Press, *Oxford*, UK, 1995.

2- Self, M. and Ripken, J. F., Steady state –cavity studies in free-jet water tunnel. St. Anthony Falls Hydrodynamic Laboratory Report 47, 1955.

3- G. Wang, S.M. Ostoja, Large eddy simulation of a sheet/cloud cavitation on a NACA0015 hydrofoil, Appl. Math. Model. 31 (2007) 417–447.

4- Kunz, R.F.,Chyczewski, T., Boger, D., Stinebring, D., Gibeling, H., Govindan, T.R., "Multi-phase CFD analysis of natural and ventilated cavitation about submerged bodies". in Proceedings of FEDSM 99, 3rd ASME/JSME Joint Fluids Engineering Conference,1999.

5- Passandideh-Fard, M., Roohi, E., Transient simulations of cavitating flows using a modified volume-of-fluid (VOF) technique, *International Journal of Computational Fluid Dynamics*, Volume 22, 2008, Pages 97-114.

6- Nouri N.M., Moghimi M. and Mirsaeedi S.M.H., Numerical Simulation of Unsteady Cavitating Flow Over a Disk, Proc. IMechE, Vol.224, 2010, pp. 1245-1253

7- Baradaran Fard, M., Nikseresht, A. H., Numerical simulation of unsteady 3D cavitating flows over axisymmetric cavitators, Scientia Iranica, Transactions B: Mechanical Engineering, Volume 19, 2012, Pages 1258-1264

8- Shang, Z. Emerson, D. R. and Xiaojun Gu, Numerical investigations of cavitation around a high speed submarine using OpenFOAM with LES, International Journal of Computational Methods, Volume 9, 2012, 1250040-1250054.

9- Roohi, E., Zahiri, A. P., Passandideh-Fard, M., Numerical Simulation of Cavitation around a Two-Dimensional Hydrofoil Using VOF Method and LES

Turbulence Model, Applied Mathematical Modeling, DOI: 10.1016/j.apm.2012.09.002.

10- Morgut, M., Nobile, E., "Numerical Predictions of Cavitating Flow around Model Scale Propellers by CFD and Advanced Model Calibration", International Journal of Rotating Machinery, Vol. 2012, 618180, 2012.

11- Shang, Z., Numerical investigations of supercavitation around blunt bodies of submarine shape, *Applied Mathematical Modeling*, DIO:10.1016/j.apm.2013.04.009.

12- Kunz, R. F., Boger, D. A., Stinebring, D. R., Chyczewski, T. S., Gibeling, H. J., Venkateswaran, S. and Govindan, T. R. A preconditioned Navier-Stokes method for two-phase flows with application to cavitation prediction. *J. Comput. Fluids*, 2000, 29, 849-875

13- G.H. Schnerr, J. Sauer, Physical and numerical modelling of unsteady cavitation dynamics, in: Proceedings of 4th International Conference on Multiphase Flow, New Orleans, USA, 2001.

14- Brennan, C., "Fundamentals of Multiphase Flows", Cambridge Univ. Press, Cambridge, UK. 2005.

15- Bensow, R. E. and Bark, G., "Simulating cavitating flows with LES in OpenFOAM" V European Conference on Computational Fluid Dynamics, pp. 14-17 June, 2010.

16- Lu, N.X., "Large Eddy Simulation of Cavitating Flow on Hydrofoils" licentiate of engineering thesis, Department of Shipping and Marine Technology, Chalmers University of Technology, Göteborg, Sweden, 2010.

17- Sagaut T, P., 2006, "Large Eddy Simulation for Incompressible Flows" Springer, New York, 3rd edition.

18- Fureby, C., and Grinstein, F., "Large Eddy Simulation of High-Reynolds Number Free and Wall-Bounded Flows" journal of Computational Physics,Vol.181, pp. 68–97, 2002.

19- Franc, J.P. and Michel J.M., Fundamentals of Cavitation, 115 Kluwer Academic Publisher, Netherlands Section: 6 (2004)